Leukemia
https://doi.org/10.1038/s41375-019-0505-x

ARTICLE

Acute myeloid leukemia

The neuropeptide receptor calcitonin receptor-like (CALCRL) is a potential therapeutic target in acute myeloid leukemia

Linus Angenendt[1] · Eike Bormann[2] · Caroline Pabst[3] · Vijay Alla[1] · Dennis Görlich[2] · Leonie Braun[1] · Kim Dohlich[1] · Christian Schwöppe[1] · Stefan K. Bohlander[4] · Maria Francisca Arteaga[1] · Klaus Wethmar[1] · Wolfgang Hartmann[5] · Adrian Angenendt[6] · Torsten Kessler[1] · Rolf M. Mesters[1] · Matthias Stelljes[1] · Maja Rothenberg-Thurley[7] · Karsten Spiekermann[7] · Josée Hébert[8,9,10,11] · Guy Sauvageau[8,9,10,11] · Peter J. M. Valk[12] · Bob Löwenberg[12] · Hubert Serve[13] · Carsten Müller-Tidow[3] · Georg Lenz[1] · Bernhard J. Wörmann[14] · M. Christina Sauerland[2] · Wolfgang Hiddemann[7] · Wolfgang E. Berdel[1] · Utz Krug[15] · Klaus H. Metzeler[7] · Jan-Henrik Mikesch[1] · Tobias Herold[7,16] · Christoph Schliemann[1]

Received: 11 March 2019 / Revised: 12 April 2019 / Accepted: 18 April 2019

Abstract

Calcitonin receptor-like (CALCRL) is a G-protein-coupled neuropeptide receptor involved in the regulation of blood pressure, angiogenesis, cell proliferation, and apoptosis, and is currently emerging as a novel target for the treatment of migraine. This study characterizes the role of CALCRL in acute myeloid leukemia (AML). We analyzed CALCRL expression in collectively more than 1500 well-characterized AML patients from five international cohorts (AMLCG, HOVON, TCGA, Leucegene, and UKM) and evaluated associations with survival. In the AMLCG analytic cohort, increasing transcript levels of *CALCRL* were associated with decreasing complete remission rates (71.5%, 53.7%, 49.6% for low, intermediate, high *CALCRL* expression), 5-year overall (43.1%, 26.2%, 7.1%), and event-free survival (29.9%, 15.8%, 4.7%) (all $P < 0.001$). *CALCRL* levels remained associated with all endpoints on multivariable regression analyses. The prognostic impact was confirmed in all validation sets. Genes highly expressed in *CALCRL*^{high} AML were significantly enriched in leukemic stem cell signatures and *CALCRL* levels were positively linked to the engraftment capacity of primary patient samples in immunocompromised mice. CRISPR-Cas9-mediated knockout of *CALCRL* significantly impaired colony formation in human myeloid leukemia cell lines. Overall, our study demonstrates that CALCRL predicts outcome beyond existing risk factors and is a potential therapeutic target in AML.

Introduction

The *calcitonin receptor-like* (*CALCRL*) gene, located on chromosome 2q32.1, encodes for a seven-transmembrane G-protein-coupled receptor that mediates the pleiotropic effects of calcitonin gene-related peptide (CGRP) and adrenomedullin (ADM), two structurally related neuropeptides originally described as potent vasodilators [1, 2]. Beyond blood pressure regulation, CALCRL is involved in a variety of key biological processes, including cell proliferation, modulation of apoptosis, vascular biology, and inflammation [3–5], and is currently emerging as a novel target for the therapy of migraine [6, 7]. In solid tumors, antibody-mediated inhibition of CALCRL signaling has been demonstrated to reduce tumor growth via disruption of angiogenesis or via direct antiproliferative effects on cancer cells [8–12]. Interestingly, it was further shown that

These authors contributed equally: Linus Angenendt, Eike Bormann

These authors contributed equally: Tobias Herold, Christoph Schliemann

Supplementary information The online version of this article (https://doi.org/10.1038/s41375-019-0505-x) contains supplementary material, which is available to authorized users.

✉ Linus Angenendt
linus.angenendt@ukmuenster.de

✉ Tobias Herold
tobias.herold@med.uni-muenchen.de

✉ Christoph Schliemann
christoph.schliemann@ukmuenster.de

Extended author information available on the last page of the article

Published online: 10 June 2019

CALCRL is expressed in normal CD34$^+$ hematopoietic progenitors and that CGRP and ADM directly act on CD34$^+$ cells to promote colony formation in vitro, indicating a functional role of CALCRL in physiological myelopoiesis [13–16].

However, the role of CALCRL in malignant hematopoiesis is unknown. Here, we comprehensively investigated the impact of CALCRL expression levels on clinical outcome in more than 1500 acute myeloid leukemia (AML) patients on transcript or protein level and provide biological insights that suggest targeting of the CALCRL pathway as a novel therapeutic strategy in AML.

Methods

Patients, samples, and treatment

CALCRL gene expression was analyzed in diagnostic samples from 492 AML patients, who received intensive age-adapted chemotherapy within the AMLCG99 trial of the German AML Cooperative Group (analytic cohort; NCT00266136; Table 1) [17]. A Dutch-Belgian Hematology Oncology Cooperative Group (HOVON) cohort of intensively treated patients with de novo AML ($n = 400$) [18, 19], The Cancer Genome Atlas (TCGA) AML cohort ($n = 157$, intensively treated subcohort $n = 125$) [20], and a clinically annotated subcohort of the Canadian Leucegene 415 AML patients cohort ($n = 263$) [21] served as validation sets (Supplementary Tables 1 and 2). Apart from survival data, clinicopathological variables were not available from the Leucegene cohort. CALCRL protein expression was analyzed on tissue microarrays (TMA) of pretreatment bone marrow (BM) trephines from 190 AML patients receiving intensive chemotherapy at the University Hospital Münster (UKM; Supplementary Table 3). Patients with acute promyelocytic leukemia or myelodysplastic syndromes (except the former RAEB-t subtype) were excluded from all cohorts. A study profile is shown in Supplementary Fig. 1.

Procedures

Samples from the analytic cohort were analyzed using Affymetrix HG-U133 A, B, and Plus 2.0 microarrays (Affymetrix, Santa Clara, CA) as described (GSE37642; Supplementary Methods) [22]. Expression data from the HOVON cohort generated with Affymetrix HG-U133 Plus 2.0 chips were preprocessed as above and clinical annotations were provided by the authors (GSE6891) [18]. TCGA RNAseq and clinical data were downloaded from cBioPortal on 25 July 2017 [20]. The Leucegene cohort and methodology for RNAseq have been described previously

Table 1 Pretreatment characteristics of 492 AML patients of the AMLCG analytic cohort, categorized as *CALCRL*^{low}, *CALCRL*^{int} and *CALCRL*^{high}

Variables	*CALCRL*			
	Low	Intermediate	High	*P* value
N	123	246	123	
Age, years				**<0.0001**[a]
Median (range)	48 (19–83)	58 (18–85)	63 (20–79)	
Sex, *n* (%)				0.85[b]
Male	59 (48.0)	125 (50.8)	63 (51.2)	
Female	64 (52.0)	121 (49.2)	60 (48.8)	
AML type, *n* (%)				0.10[b]
De novo	111 (90.2)	201 (81.7)	105 (85.4)	
s-AML	6 (4.9)	33 (13.4)	10 (8.1)	
t-AML	6 (4.9)	12 (4.9)	8 (6.5)	
FAB, *n* (%)				**<0.0001**[b]
M0	2 (1.6)	7 (2.9)	12 (9.8)	
M1	19 (15.6)	43 (17.6)	45 (36.9)	
M2	41 (33.6)	88 (36.1)	30 (24.6)	
M4	35 (28.7)	60 (24.6)	21 (17.2)	
M5	23 (18.9)	32 (13.1)	7 (5.7)	
M6	2 (1.6)	12 (4.9)	6 (4.9)	
M7	0 (0.0)	2 (0.8)	1 (0.8)	
WBC, $\times 10^9$/l				0.16[a]
Median (range)	24.4 (0.9–280.1)	16.0 (0.1–666.0)	21.8 (0.9–486.0)	
LDH level, U/l				**0.0017**[a]
Median (range)	558 (127–4613)	428 (76–3630)	436 (87–4610)	
Hb, g/dl				**0.024**[a]
Median (range)	9.4 (3.6–14.3)	9.0 (3.5–14.2)	8.8 (4.0–15.4)	
Platelets, $\times 10^9$/l				0.53[a]
Median (range)	44 (6–406)	53 (0–1760)	53 (4–670)	
BM blasts, %				**0.036**[a]
Median (range)	80 (20–100)	80 (13–100)	85 (21–100)	
Cytogenetics[c], *n* (%)				
t(8;21)	12 (9.8)	16 (6.5)	0 (0.0)	**0.0032**[b]
inv(16)/t(16;16)	15 (12.2)	19 (7.7)	3 (2.4)	**0.015**[b]
normal	49 (39.8)	100 (40.7)	56 (45.5)	0.60[b]
t(9;11)	11 (8.9)	7 (2.9)	1 (0.8)	**0.0031**[d]
t(6;9)	1 (0.8)	3 (1.2)	0 (0.0)	0.81[d]
t(9;22)	–	–	–	
t(*v*;11q23)	7 (5.7)	6 (2.4)	3 (2.4)	0.26[d]
inv(3)/t(3;3)	2 (1.6)	3 (1.2)	8 (6.5)	**0.013**[d]
−5/del(5q)	4 (3.3)	21 (8.5)	19 (15.5)	**0.0035**[b]
−7	4 (3.3)	15 (6.1)	14 (11.4)	**0.034**[b]
−17/abn(17p)	2 (1.6)	8 (3.3)	12 (9.8)	**0.0036**[b]
complex	8 (6.5)	31 (12.6)	27 (22.0)	**0.0016**[b]
monosomal	5 (4.1)	19 (7.7)	22 (17.9)	**0.0005**[b]
other	16 (13.0)	49 (19.9)	21 (17.1)	0.25[b]
FLT3-ITD, *n* (%)				0.18[b]
Present	24 (20.5)	70 (29.7)	31 (25.8)	**0.021**[b]
High allelic ratio (≥0.5)	10 (41.7)	39 (54.9)	24 (77.4)	
Low allelic ratio (<0.5)	14 (58.3)	32 (45.1)	7 (22.6)	
Absent	93 (79.5)	166 (70.3)	89 (74.2)	

Table 1 (continued)

Variables	*CALCRL*			
	Low	Intermediate	High	*P* value
NPM1, *n* (%)				0.51[b]
Mutated	35 (29.9)	65 (27.5)	28 (23.3)	
Wild type	82 (70.1)	171 (72.5)	92 (76.7)	
NPM1/*FLT3*-ITD, *n* (%)				**0.0070**[b]
$NPM1^{mut}$/$FLT3\text{-}ITD^{neg/low}$	28 (23.9)	40 (17.0)	9 (7.5)	
$NPM1^{mut}$/$FLT3\text{-}ITD^{high}$	7 (6.0)	25 (10.6)	19 (15.8)	
$NPM1^{wt}$/$FLT3\text{-}ITD^{neg/low}$	79 (67.5)	157 (66.5)	87 (72.5)	
$NPM1^{wt}$/$FLT3\text{-}ITD^{high}$	3 (2.6)	14 (5.9)	5 (4.2)	
CEBPA, *n* (%)				**0.0029**[d]
Double mutated	10 (9.9)	3 (1.5)	4 (4.0)	
Wild type or single mutated	91 (90.1)	201 (98.5)	95 (96.0)	
RUNX1, *n* (%)				**<0.0001**[b]
Mutated	12 (10.3)	27 (11.4)	33 (27.5)	
Wild type	105 (89.7)	209 (88.6)	87 (72.5)	
ASXL1, *n* (%)				0.57[b]
Mutated	10 (8.6)	29 (12.3)	14 (11.7)	
Wild type	107 (91.4)	207 (87.7)	106 (88.3)	
TP53, *n* (%)				**0.0017**[b]
Mutated	7 (6.0)	23 (9.8)	24 (20.0)	
Wild type	110 (94.0)	213 (90.2)	96 (80.0)	
Cytogenetic and molecular risk[e], *n* (%)				**<0.0001**[b]
Favorable	65 (54.6)	78 (32.2)	16 (13.3)	
Intermediate	26 (21.9)	67 (27.7)	28 (23.3)	
Adverse	28 (23.5)	97 (40.1)	76 (63.3)	

AML acute myeloid leukemia, *s-AML* secondary AML, *t-AML* therapy-related AML, *FAB* French-American-British classification, *WBC* white blood cell count, *LDH* lactate dehydrogenase, *Hb* hemoglobin, *BM* bone marrow, *FLT3-ITD* internal tandem duplication of the *FLT3* gene, *NPM1* nucleophosmin-1, *CEPBA* CCAAT/enhancer binding protein α, *RUNX1* Runt-related transcription factor 1, *ASXL1* additional sex combs like 1, *TP53* tumor protein p53. Significant *P* values are marked in bold

[a]Kruskal–Wallis test

[b]χ^2 test

[c]Patients may be counted more than once in cases with two or more coexisting cytogenetic abnormalities

[d]Fisher's exact test

[e]According to European LeukemiaNet 2017 guidelines

[21] and survival data have been provided by the authors. Gene set enrichment analysis (GSEA) was performed using the "C2" collection of the Molecular Signatures Database (http://software.broadinstitute.org/gsea/msigdb/) consisting of 4731 gene sets curated from various sources.

CALCRL immunohistochemistry (IHC) was visually scored by two investigators using an H-score. Visual scores were then compared to semiautomatic digital scoring using TMARKER (v2.162), an application that uses machine learning for computer aided cell counting and staining estimation [23].

CALCRL gene expression was determined in sorted normal human BM, cord blood, and peripheral blood cell populations as well as in samples of 56 AML patients with low, intermediate, and high leukemia stem cell (LSC) frequencies, as determined by engraftment capacity in NSG mice [24].

CRISPR-Cas9-mediated knockout of *CALCRL* was performed in human myeloid leukemia cell lines by lentiviral transduction with lentiCRISPR v2 containing sgRNAs targeting human *CALCRL*. After antibiotic selection, cells were cultured in methylcellulose and colonies were counted after 10 days.

Statistical analyses

Time-to-event and response variables were defined as described [18, 20, 22] or followed the 2017 European LeukemiaNet (ELN) recommendations [25]. Follow-up time was calculated by reverse Kaplan–Meier method. We used restricted cubic splines with three knots to delineate potential non-linear associations of *CALCRL* with outcome. In each cohort, the lowest *CALCRL* expression value was chosen as a reference category for calculation of the hazard (HR) and odds ratios (OR). Cox proportional hazards models were fitted to estimate the effect of an interquartile range increase in *CALCRL* expression as a continuous term on overall (OS) and event-free survival (EFS), as implemented in the *rms* package. Likewise, logistic regression models were fitted to assess associations with achievement of complete remission (CR). To visualize survival probabilities with the Kaplan–Meier estimator cohorts were trichotomized by *CALCRL* expression levels: low (Q1), intermediate (Q2/3), and high (Q4). Survival probabilities were compared using log-rank tests and are given at 5 years. Clinical and molecular baseline variables were compared between *CALCRL* expression groups using χ^2 or Fisher's exact test for categorical and the Kruskal–Wallis test for continuous variables. Potential heterogeneity of prognostic effects across subgroups was examined with Cox proportional hazards models and Wald test for interaction.

Multivariable Cox proportional hazards models were generated to assess statistical significance of prognostic factors with respect to OS and EFS, and multivariable logistic regression models to assess achievement of CR. Besides *CALCRL* expression, age, white blood cell (WBC) count, lactate dehydrogenase (LDH) activity, and cytogenetic and molecular risk factors were entered in the full multivariable models. Multicollinearity among predictors was examined using variance inflation factors (VIF). The proportional hazards assumption was verified for each

variable individually by inspection of scaled Schoenfeld residuals and χ^2 test for correlation of residuals with transformed survival time (all $P > 0.05$). In addition, we used elastic net penalized regression with 100-fold repeated tenfold cross-validation to identify sparse prognostic models in the context of correlated predictor variables [26]. Missing data were not imputed. Two-sided P values <0.05 were considered significant. Analyses were performed using SAS for Windows, version 9.4 (SAS Institute, Cary, North Carolina, USA) and R software, version 3.5.1 (www.r-project.org).

Results

The median follow-up time for AMLCG patients was 8.7 years (IQR 7.3–10.5). In restricted cubic spline analyses the OR for achievement of CR decreased, whereas HRs for death or experiencing an event increased over the whole range of *CALCRL* expression values (Fig. 1; Supplementary Fig. 2). An increase of *CALCRL* expression from the 25th to 75th percentile was associated with inferior OS (hazard ratio [HR], 1.60; 95% confidence interval [CI], 1.33–1.93; $P < 0.0001$), EFS (HR, 1.58; 95% CI, 1.33–1.89; $P < 0.0001$), and CR rate (odds ratio [OR], 0.57; 95% CI, 0.41–0.79; $P < 0.0010$). As a categorical variable, *CALCRL*^{low} cases showed a significantly higher CR rate compared with *CALCRL*^{int} or *CALCRL*^{high} patients (71.5%, 53.7%, and 49.6% for low, intermediate, and high *CALCRL* expression; $P = 0.0007$). Progressively higher *CALCRL* levels predicted poorer OS (43.1%, 26.2%, 7.1% for low, intermediate, and high *CALCRL* expression; $P < 0.0001$) and EFS (29.9%, 15.8%, 4.7%; $P < 0.0001$) (Fig. 1). When censoring at allogeneic HSCT, *CALCRL* levels remained significantly associated with OS and EFS (both $P < 0.0001$; Supplementary Fig. 3).

Table 1 lists the baseline characteristics of the 492 patients from the AMLCG analytic cohort categorized by trichotomized *CALCRL* expression. Higher *CALCRL* transcript levels significantly associated with older age. *CALCRL*^{high} expression significantly co-occurred with immature cytomorphology (FAB M0/1), and *CALCRL*^{low} expression with monocytic differentiation (M4/M5; $P <$ 0.0001). Patients with *CALCRL*^{high} AML had higher BM blast counts, but lower LDH levels. High *CALCRL* expression associated with complex karyotype, monosomal karyotype, inv(3)/t(3;3), −5/del(5q), −7 and −17/abn(17p) (Table 1; Supplementary Fig. 4). In contrast, core-binding factor (CBF) and 11q23 rearrangements were underrepresented among *CALCRL*^{high} patients. There was no association between *CALCRL* expression and *FLT3*-ITD or *NPM1* mutations when analyzed separately. However, in *NPM1*^{mut} AML, lower *CALCRL* levels were associated with *FLT3*-ITD$^{neg/low}$, whereas higher levels co-occurred with *FLT3*-ITD^{high} status. *CALCRL*^{high} AML more frequently harbored *RUNX1* and *TP53*, but fewer biallelic *CEBPA* (bi*CEBPA*) mutations. Taken together, *CALCRL*^{high} expressers were more frequently classified in the adverse ELN 2017 risk group and *CALCRL*^{high} status correlated with most of the individual alterations defining this category (except t(*v*;11q23) and *ASXL1* mutations; t(6;9) and t(9;22) not evaluable due to low frequencies). In turn, more than half of the patients with *CALCRL*^{low} AML but only 13.3% of the *CALCRL*^{high} expressers had a favorable-risk profile.

In multivariable analyses, the likelihood of achieving a CR for *CALCRL*^{low} expressers was more than double that of *CALCRL*^{int} or *CALCRL*^{high} expressers (odds ratio [OR], 2.29; 95% confidence interval [CI], 1.30–4.05; $P = 0.0052$; Table 2). *CALCRL* levels predicted OS ($P = 0.024$) and EFS ($P = 0.0091$), after adjusting for established risk factors, that remained in the final model after backward elimination, including age and cytogenetic and molecular risk factors from the ELN 2017 criteria. *CALCRL*^{low} expressers had a one-third reduced risk of induction failure, relapse, or death (hazard ratio [HR] *CALCRL*^{low} vs *CALCRL*^{int}, 0.66; 95% CI, 0.49–0.88; $P = 0.0048$). We found only low to moderate collinearity among predictors with a median VIF of 1.2 (range 1.1–1.7). In a second multivariable model using elastic net regression for selection of prognostic factors from 21 genetic and clinical risk factors, *CALCRL* expression consistently remained among the selected variables (Supplementary Fig. 5).

In exploratory subgroup analyses, we found no significant heterogeneity of the prognostic effect of *CALCRL* expression on OS across the larger clinicopathological subgroups including age (<60 years vs ≥60 years) and ELN 2017 genetic risk categories (Supplementary Fig. 6). However, the hazard risk of death associated with high *CALCRL* expression seemed to be higher in younger than in older patients (HR 2.57 vs 1.79 for <60 vs ≥60 years; $P =$ 0.13 for interaction) with a similar hazard risk of experiencing an event (2.59 vs 1.39 for <60 vs ≥60 years; $P =$ 0.048 for interaction) (Supplementary Fig. 7). A more detailed analysis of *CALCRL* expression in subgroups by age can be found in Supplementary Tables 4 and 5 and Supplementary Fig. 8. In smaller genetic subgroups, we identified significant heterogeneity of the prognostic effect of *CALCRL* expression on OS for patients with −7 ($P =$ 0.011 for interaction) and monosomal karyotype ($P = 0.030$ for interaction). These interactions did not remain significant when analyzing subgroup effects on EFS (Supplementary Fig. 7).

To validate our findings, we investigated *CALCRL* gene expression in three independent cohorts. As a continuous variable and when trichotomized as above, higher *CALCRL* levels were consistently associated with an adverse outcome

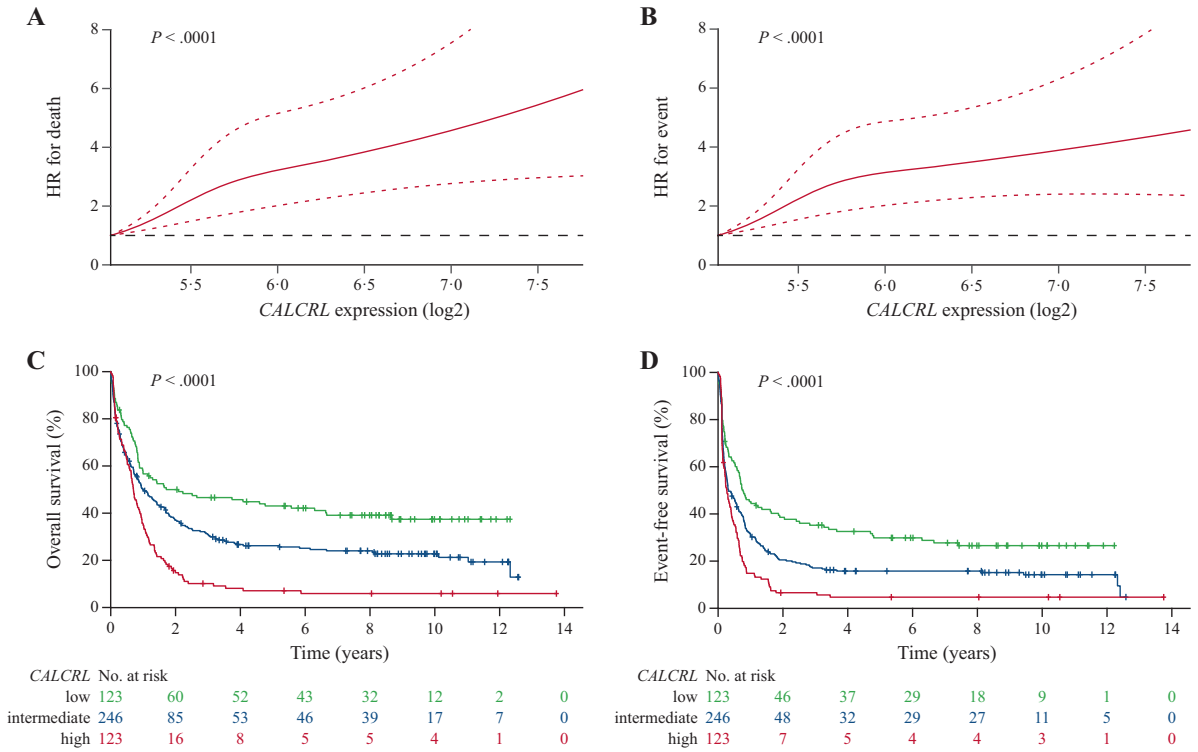

Fig. 1 *CALCRL* gene expression and survival in the AMLCG analytic cohort. Overall survival (**a**, **c**) and event-free survival (**b**, **d**) according to continuous (**a**, **b**) and trichotomized (**c**, **d**) microarray-based *CALCRL* expression levels. Splines (**a**, **b**) are shown with a 95% confidence interval. The horizontal dotted line indicates a hazard ratio of 1

in the HOVON, TCGA (intensively treated subcohort), and Leucegene validation sets (Fig. 2). Again, *CALCRL* remained independently associated with OS and EFS in the HOVON ($P = 0.014$ and 0.041) and in the TCGA cohort ($P = 0.014$ and 0.0014) and consistently remained among the predictors in elastic net regression analyses (Supplementary Tables 6 and 7; Supplementary Fig. 5). Variables other than OS were not available for the Leucegene dataset.

CALCRL protein expression was higher in AML as compared to normal BM ($P < 0.0001$; Fig. 3a, c). The median follow-up for patients of the UKM cohort was 3.2 years (IQR 1.6–4.6). When modeled as a continuous variable or when trichotomized as above, visually assessed CALCRL H-scores were inversely correlated with CR rate (70.2%, 58.1%, 36.7%; $P = 0.0034$), OS (62.5%, 38.8%, 17.1%; $P < 0.0001$), and EFS (30.1%, 19.2%, 5.0%; $P = 0.0002$; Fig. 3b–e; Supplementary Fig. 10) and remained associated with all endpoints in multivariable analyses (Supplementary Table 8). CALCRL remained among the selected predictors in multivariable elastic net regression (Supplementary Fig. 5). Computer-assisted digital quantification of CALCRL expression was highly correlated to visual scoring ($r = 0.83$; $P < 0.0001$; Supplementary Fig. 11) and digital H-scores produced comparable results in Cox regression models (Supplementary Table 9).

CALCRL^{high} status was significantly ($P < 0.0001$) associated with the differential expression of 964 genes in the AMLCG cohort (193 up- and 771 downregulated). Figure 4a shows a heatmap of the 200 most significantly regulated genes. Among others (Supplementary Table 10), we observed a positive correlation of *CALCRL* with *MN1* and *BAALC* expression, which have been extensively characterized in the context of leukaemogenesis and prognosis in AML [27–32]. In multivariable models including *MN1*, *BAALC*, and *CALCRL* expression as covariables, however, only *CALCRL* retained prognostic significance for survival in the full AMLCG, HOVON, and TCGA cohorts, and in the CN-AML subcohorts (Supplementary Tables 11 and 12), whereas *MN1* and *BAALC* became uninformative ($P > 0.05$). *CALCRL* also correlated with *BCAT1*, an aminotransferase for branched-chain amino acids that contributes to the differentiation block in AML [33]. Another gene, the transcription factor *ZNF521*, has been recently identified as a regulator of stem cell function and *MLL-AF9* leukemogenesis [34]. In turn, there was an inverse relationship of *CALCRL* expression with genes related to myeloid differentiation such as *AZU1*, *MPO*, *ELANE*, or *CTSG*. In GSEA, genes associated with *CALCRL*^{high} AML were significantly enriched in HSC, LSC, and cell adhesion signatures (Supplementary Table 13).

Table 2 Multivariable regression analyses in the AMLCG analytic cohort

Variables in final models	OR/HR	95% CI	*P* value
Complete remission			
Age: ≥60 vs <60 years	0.59	0.38–0.92	**0.021**
Karyotype[a]			**0.0001**
Favorable vs intermediate risk	1.19	0.56–2.51	**0.041**
Adverse vs intermediate risk	0.31	0.17–0.55	**<0.0001**
NPM1/*FLT3*-ITD mutation status[b]			0.051
Low vs intermediate risk	1.71	0.90–3.26	**0.015**
High vs intermediate risk	0.41	0.14–1.18	**0.034**
RUNX1: mutated vs wild type	0.53	0.29–0.99	**0.045**
CALCRL expression			**0.015**
Low vs intermediate	2.29	1.30–4.05	**0.0052**
High vs intermediate	1.07	0.63–1.83	0.20
Overall survival			
Age: ≥60 vs <60 years	1.80	1.40–2.30	**<0.0001**
WBC: ≥50 vs <50 × 10^9/l	1.33	1.00–1.75	**0.047**
LDH: ≥700 vs <700 U/l	1.41	1.08–1.86	**0.012**
Karyotype[a]			**0.0003**
Favorable vs intermediate risk	0.38	0.23–0.63	**0.0002**
Adverse vs intermediate risk	1.15	0.82–1.60	0.43
NPM1/*FLT3*-ITD mutation status[b]			**0.0002**
Low vs intermediate risk	0.46	0.32–0.67	**<0.0001**
High vs intermediate risk	1.12	0.66–1.92	0.67
CEPBA: double mutated vs wild type or single mutated	0.51	0.24–1.06	0.070
RUNX1: mutated vs wild type	1.64	1.18–2.29	**0.0035**
TP53: mutated vs wild type	2.18	1.41–3.36	**0.0004**
CALCRL expression			**0.024**
Low vs intermediate	0.71	0.51–0.98	**0.038**
High vs intermediate	1.16	0.88–1.54	0.30
Event-free survival			
Age: ≥60 vs <60 years	1.62	1.28–2.05	**<0.0001**
WBC: ≥50 vs <50 × 10^9/l	1.43	1.12–1.82	**0.0039**
Type of AML			**0.024**
s-AML vs de novo	0.87	0.58–1.31	0.51
t-AML vs de novo	2.08	1.20–3.61	**0.0094**
Karyotype[a]			**<0.0001**
Favorable vs intermediate risk	0.55	0.36–0.84	**0.0053**
Adverse vs intermediate risk	1.85	1.33–2.58	**0.0003**
NPM1/*FLT3*-ITD mutation status[b]			**0.0023**
Low vs intermediate risk	0.60	0.43–0.84	**0.0029**
High vs intermediate risk	1.52	0.92–2.50	0.10
RUNX1: mutated vs wild type	1.71	1.24–2.34	**0.0009**
TP53: mutated vs wild type	1.52	0.98–2.36	0.060
CALCRL expression			**0.0091**
Low vs intermediate	0.66	0.49–0.88	**0.0048**
High vs intermediate	1.05	0.79–1.38	0.75

Odds ratios (OR) greater or less than 1.0 indicate higher or lower CR rates, respectively, for the first category listed. Hazard ratios (HR) greater or less than 1.0 indicate an increased or decreased risk, respectively, of an event for the first category listed. Significant *P* values are marked in bold

AML acute myeloid leukemia, *s-AML* secondary AML, *t-AML* therapy-related AML, *WBC* white blood cell count, *LDH* lactate dehydrogenase, *NPM1* nucleophosmin-1, *FLT3-ITD* internal tandem duplication of the *FLT3* gene, *CEPBA* CCAAT/enhancer binding protein α, *RUNX1* Runt-related transcription factor 1, *ASXL1* additional sex combs like 1, *TP53* tumor protein p53, *CALCRL* calcitonin receptor-like

[a]Cytogenetic risk groups according to ELN 2017 definitions

[b]The low-risk group is defined as *NPM1*^{mut}/*FLT3*-ITD$^{neg/low}$, the intermediate-risk group is defined as *NPM1*^{mut}/*FLT3*-ITD^{high} or *NPM1*^{wt}/*FLT3*-ITD$^{neg/low}$, and the high-risk group is defined as *NPM1*^{wt}/*FLT3*-ITD^{high}, in accordance with ELN 2017 definitions

Variables considered in the models for CR, OS, and EFS were age (≥60 vs <60 years), WBC (≥50 vs <50 × 10^9/l), LDH (≥700 vs <700 U/l), type of AML (de novo vs s-AML vs t-AML), karyotype (favorable vs intermediate vs adverse risk)[a], *NPM1*/*FLT3*-ITD mutation status (low vs intermediate vs high risk)[b], *CEBPA* (double mutated vs wild type or single mutated), *RUNX1* (mutated vs wild type), *ASXL1* (mutated vs wild type), *TP53* (mutated vs wild type), and *CALCRL* (low vs intermediate vs high)

When analyzing normal hematopoietic cells, *CALCRL* expression was significantly increased in the CD34$^+$ compartment, with higher expression in immature CD34$^+$/CD45RA$^-$ cells compared with committed CD34$^+$/CD33$^+$ myeloid progenitors but was virtually absent in mature myeloid cells (Fig. 4b). In AML, when analyzing 56 patient-derived specimens, *CALCRL* levels were positively linked to a sample's LSC frequency and leukemogenic potential in immunocompromised mice (Fig. 4c). CRISPR-Cas9-mediated knockout of *CALCRL* resulted in a significant reduction of colony formation capacity of three myeloid leukemia cell lines as compared to controls (Fig. 4d; Supplementary Fig. 13). Despite its correlation with LSC signatures, *CALCRL* remained associated with outcome after adjusting for the 17-gene stemness (LSC17) score (Supplementary Table 14) [35]. We found a significant interaction of low vs high *CALCRL* expression and the LSC17 score ($P = 0.026$ for interaction). *CALCRL* further stratified survival in LSC17-classified low-risk patients, with 5-year OS rates differing by more than 40% between LSC17^{low}/*CALCRL*^{low} and LSC17^{low}/*CALCRL*^{high} patients (Fig. 4e–g; Supplementary Fig. 14).

Discussion

We report a consistent relationship of increasing *CALCRL* expression levels with poor outcome across several independent cohorts of intensively treated AML patients and across different measurement platforms. Obviously, high *CALCRL* overlapped with unfavorable genetics, including

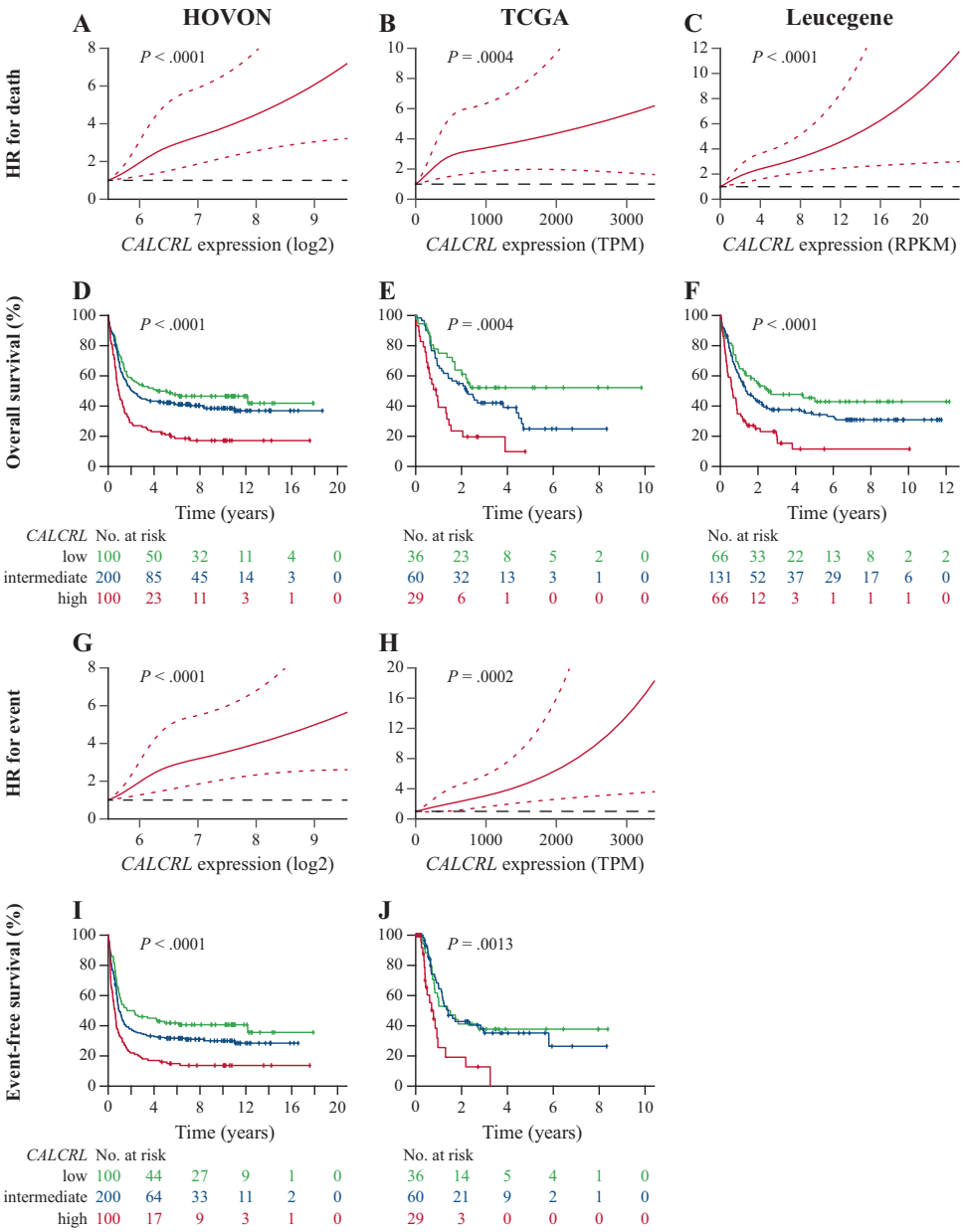

Fig. 2 *CALCRL* gene expression and survival in the HOVON, TCGA, and Leucegene validation cohorts. Overall (**a**–**f**) and event-free survival (**g**–**j**) according to *CALCRL* transcript levels in the HOVON cohort (**a**, **d**, **g**, **i**), the intensively treated TCGA subcohort (**b**, **e**, **h**, **j**), and the Leucegene cohort (**c**, **f**). EFS data were not available for the Leucegene cohort. Splines (**a**–**c**, **g**, **h**) are shown with a 95% confidence interval. The horizontal dotted lines indicate a hazard ratio of 1

complex and monosomal karyotypes, −5/del(5q), −7, −17/abn(17p), inv(3)/t(3;3) and *RUNX1* and *TP53* mutations, suggesting that *CALCRL* might be part of a shared network induced by diverse genetic events. In turn, low *CALCRL* expression associated with CBF cytogenetics, bi*CEBPA* mutations and *NPM1*^{mut}/*FLT3*-ITD$^{neg/low}$ status. However, the prognostic impact of *CALCRL* does not merely reflect its correlation with established risk factors since *CALCRL* predicted a poor prognosis, even when all criteria defined in the ELN 2017 risk stratification were included as covariables in the multivariable models. Furthermore, the prognostic impact of *CALCRL* was independent from *BAALC* and *MN1* expression, which have been extensively described for their prognostic role in AML [27–32], and from the recently described 17-gene stemness score LSC17 (which does not contain *CALCRL* as a component) [35].

Allogeneic HSCT is usually recommended for transplant-eligible patients with intermediate- or adverse-risk genetics, whereas favorable-risk patients typically receive consolidation chemotherapy [25]. We found no heterogeneity of the prognostic impact of *CALCRL* expression across subgroups defined by ELN 2017 genetic risk. *CALCRL* expression might be used to further stratify genetic risk. However, the exploratory nature of these subgroup analyses demands further validation. Given the limited number of allogeneic HSCTs performed in first CR in the AMLCG study (7.4%) and our gene expression subcohort (6.3%) [17, 36], we were not able to evaluate the

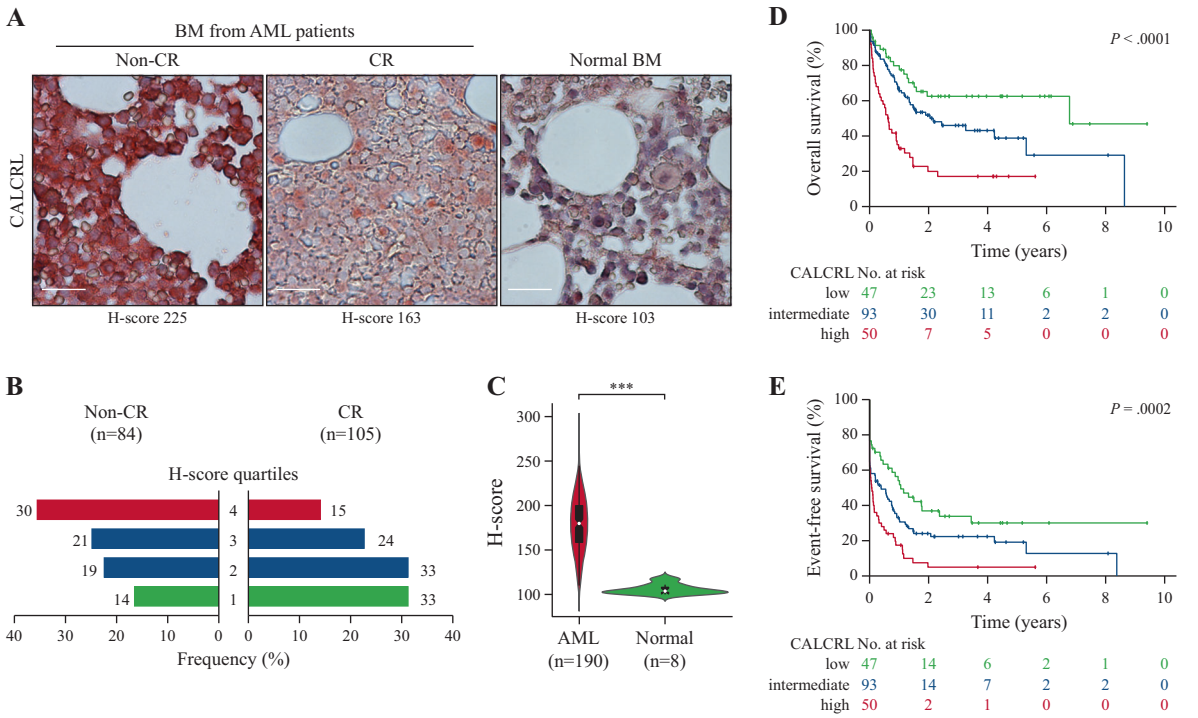

Fig. 3 CALCRL protein expression and treatment outcome in the UKM cohort. **a** Representative IHC micrographs of CALCRL expression in pretherapeutic BM from an AML patient not achieving a CR (left), a patient achieving a CR (middle), and a non-leukemic donor (right). Scale bars are 25 µm. **b** Frequency of CALCRL H-scores divided into quartiles in patients achieving a CR (left) compared to patients not achieving a CR after induction therapy (right). **c** Comparison of CALCRL H-scores between AML and normal BM. Violin plots of H-scores including a boxplot with Tukey whiskers and 95% confidence interval (notch) of the median (white dot) are shown. ***$P < 0.0001$ (Welch's *t*-test). A comparison of *CALCRL* transcript levels between AML and normal BM in an independent cohort can be found in the Supplementary Fig. 12. Overall (**d**) and event-free survival (**e**) in the UKM cohort according to trichotomized CALCRL H-scores

impact of transplantation in *CALCRL*^{high} AML, much less in *CALCRL*^{high} AML with favorable ELN risk. This should be evaluated within the framework of prospective trials incorporating risk-based stratification or randomization strategies. In any case, before quantitative measures of *CALCRL* expression can be used for clinical decision-making, standardization of the methods used to determine expression levels is necessary. Conventional IHC and visual or digital assessment of CALCRL expression in BM sections as performed in this study may represent one option for clinical translation.

Indeed, CALCRL protein expression was highly prognostic in a fifth independent cohort, further underscoring a role for CALCRL in the pathophysiology of AML. However, it is unknown how it contributes to poor chemotherapy responsiveness and aggressive disease behavior. The CALCRL pathway has been characterized in diverse pathophysiological conditions, including migraine [6, 7], sepsis [37], vascular disease [38] and solid tumors, where autocrine and paracrine CALCRL signaling loops stimulate the growth of tumor and/or endothelial cells [3, 8–12, 39–41]. In particular, CALCRL has been associated with stem cell functions across many tissues [42, 43], including normal hematopoiesis, where CGRP and ADM support colony formation of CALCRL+/CD34+ progenitors in vitro [13–16]. In our study, high *CALCRL* expression correlated with immature cytomorphology, with HSC and LSC gene expression signatures, and with the in vivo repopulating capacity of primary AML samples in mice. In addition, *CALCRL* knockout significantly impaired the colony-forming capacity of human myeloid leukemia cell lines, and *CALCRL* levels were higher in immature than in mature myeloid cells. Collectively, these findings point towards a role of *CALCRL* in HSCs and LSCs and suggest that high *CALCRL* expression indicates an AML phenotype at a more undifferentiated stage.

In addition, CALCRL has a role in malignancy-associated angiogenesis [9, 11, 12, 41], a process that is also involved in the pathophysiology of AML via reciprocal stimulation of leukemic and endothelial cells [44, 45] and that provides a protective niche for LSCs [46]. It has long been established that angiogenic mediators such as vascular endothelial growth factor, the angiopoietins, or, more recently, epithelial growth factor-like 7, not only act in a paracrine fashion on BM endothelial cells but also in direct autocrine loops to support leukemic blasts [47–49]. Indeed,

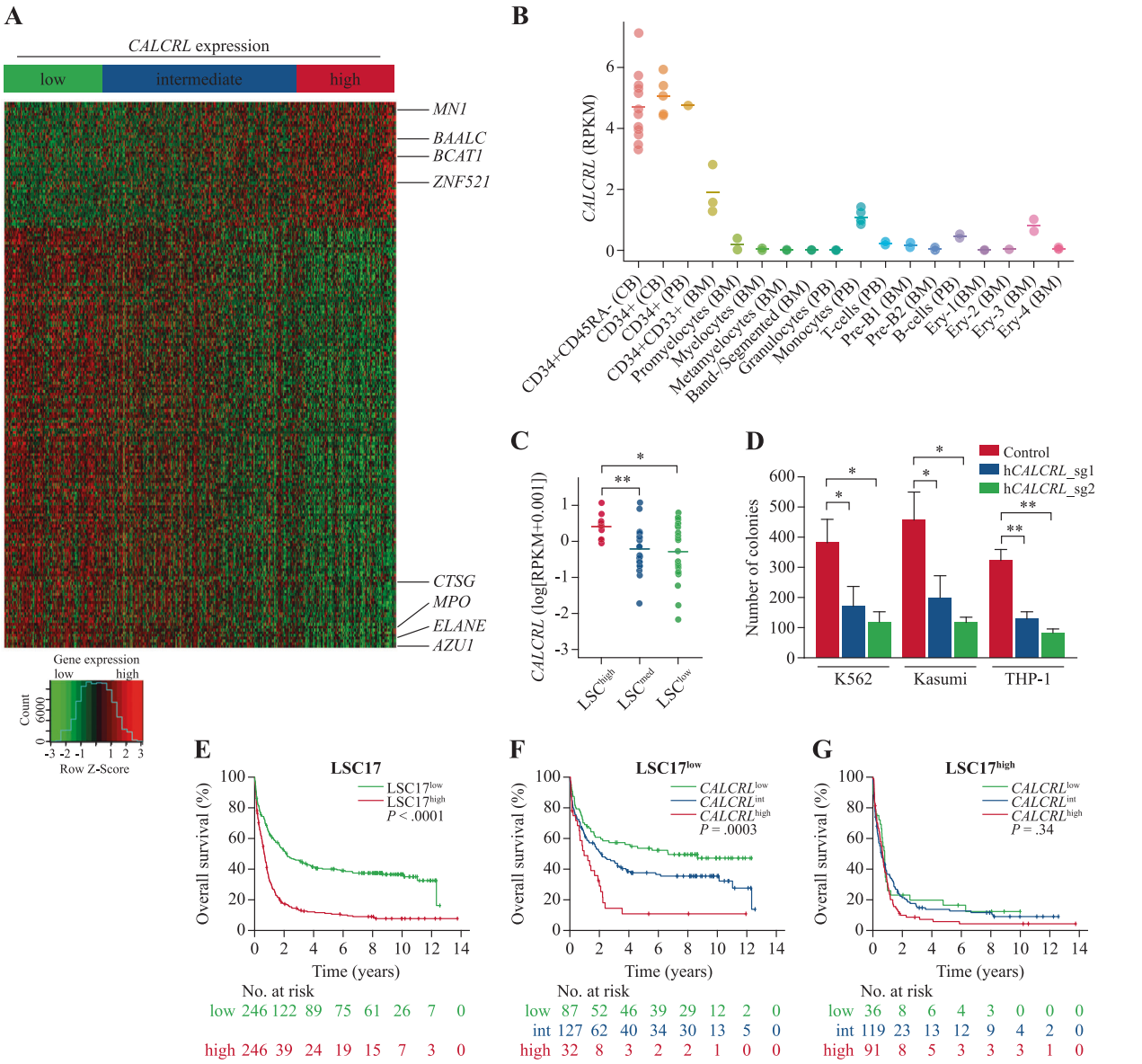

Fig. 4 Biological insights. **a** Heat map of the *CALCRL*-associated gene expression signature in the AMLCG cohort. Color-coded expression values of the 200 genes with the strongest correlation with *CALCRL* are shown, with green indicating expression below and red indicating expression above the median value for the given gene. Rows represent probe sets and columns represent patients, ordered from left to right by *CALCRL* expression. Up- and downregulated genes mentioned in the text are indicated. The complete list can be found in Supplementary Table 8. **b** *CALCRL* expression in human normal hematopoietic cell populations derived from sorted cord blood (CB), bone marrow (BM), or peripheral blood (PB) samples. **c** *CALCRL* expression in human AML samples with varying LSC frequencies. LSC frequencies were determined as described [24]. $*P < 0.05$; $**P < 0.005$ (Welch's *t*-test). **d** Impact of CRISPR-Cas9-mediated knockout of *CALCRL* on colony-forming capacity in three human myeloid leukemia cell lines using two different sgRNAs (mean ± SD, all experiments performed in triplicates, $*P < 0.05$; $**P < 0.005$ (Welch's *t*-test)). **e** Overall survival (OS) according to the LSC17 score [35] in the AMLCG cohort. **f** OS according to *CALCRL* expression in LSC17^{low} and **g** in LSC17^{high} patients

the only report investigating the CALCRL axis in leukemia suggests that autocrine ADM signaling through CALCRL could be involved in the impaired differentiation of AML cells [50], whereas in multiple myeloma, a paracrine ADM–CALCRL pathway has been identified as a major driver of the myeloma-associated angiogenic switch [51]. However, further studies will be necessary to clarify the mechanisms governing regulation of CALCRL expression, its downstream signaling pathways and biological function in the context of AML.

Importantly, the first antibodies interfering with CALCRL signaling have recently been approved for the preventive treatment of migraine [6, 7, 52]. These antibodies have so far exhibited excellent tolerability without significant hematotoxicity, rendering them attractive potential add-ons for intensive chemotherapy in AML.

Nonetheless, a better understanding of the relative vulnerabilities of LSCs and HSCs to CALCRL inhibition is required, both in the absence and presence of chemotherapy. Given that CALCRL can be activated through different ligands, it will be equally important to elucidate whether ADM or CGRP, or both, is primarily functional in leukemic as compared to normal hematopoiesis or whether one ligand is predominantly active in specific AML subtypes.

In conclusion, we identified the neuropeptide receptor CALCRL as a novel risk factor associated with stemness and poor survival in five independent AML cohorts. Further studies should more deeply characterize the functional role of CALCRL in leukemia and evaluate whether CALCRL-targeting drugs can be successfully repurposed into the context of AML.

Acknowledgements This work is dedicated to the memory of Professor Thomas Büchner. We thank all patients and clinicians participating in the trials. The help of Irina Arnhold, Mirco Witte, and Hans-Joachim Schnittler with TMA staining and analysis is gratefully acknowledged. The statistical analysis was partially funded by the José Carreras Foundation (DJCLS H 09/01f to DG). The Leucegene project is supported by the Government of Canada through Genome Canada and the Ministère de l'économie, de l'innovation et des exportations du Québec through Génome Québec, with supplementary funds from AmorChem. GS and JH are recipients of research chairs from the Canada Research Chair program and Industrielle-Alliance (Université de Montréal), respectively. The Banque de cellules leucémiques du Québec (BCLQ) is supported by grants from the Cancer Research Network of the Fonds de recherche du Québec-Santé. CP is supported by the German Cancer Aid (70111531). SKB is supported by Leukemia & Blood Cancer New Zealand and the family of Marijanna Kumerich. GL and WEB are supported by the German Research Foundation (DFG EXC 1003, Cluster of excellence "Cells in Motion"). TH and KS are supported by the Wilhelm Sander Foundation (2013.086.1 to TH and KS and 2013.086.2 to TH). TH is supported by the Physician Scientists Grant (G-509200-004) from the Helmholtz Zentrum München. C Schliemann and LA are supported by the Innovative Medical Research Fund of the University of Münster Medical School (SC211008 to CS and AN111813 to LA).

Author contributions LA, EB, TH and C Schliemann designed the study. LA, MCS, DG, AA, UK, KHM, C Schliemann, and EB performed statistical studies and analyzed the data. KW, TK, RMM, MS, HS and GL contributed to data analysis. KHM, SKB, MR-T, KS, W Hiddemann, and TH provided expression and mutational data on the AMLCG cohort. MCS, BJW, W Hiddemann, and WEB coordinated the AMLCG99 trial. JH, GS, PJMV and BL provided expression data and clinical annotations for validation cohorts. LA, LB, KD, C Schwöppe, W Hartmann, and C Schliemann characterized the UKM cohort and performed TMA stainings. CP and CMT provided expression data in hematopoietic subsets and in vivo engraftment experiments. VA, MFA and J-HM performed the CRISPR-Cas9 experiments. C Schliemann and LA wrote the manuscript. All authors interpreted the data and made the decision to submit the manuscript for publication.

Compliance with ethical standards

Conflict of interest The authors declare that they have no conflict of interest.

References

1. Kitamura K, Kangawa K, Kawamoto M, Ichiki Y, Nakamura S, Matsuo H, et al. Adrenomedullin: a novel hypotensive peptide isolated from human pheochromocytoma. Biochem Biophys Res Commun. 1993;192:553–60.
2. Brain SD, Williams TJ, Tippins JR, Morris HR, MacIntyre I. Calcitonin gene-related peptide is a potent vasodilator. Nature. 1985;313:54–6.
3. Larrayoz IM, Martinez-Herrero S, Garcia-Sanmartin J, Ochoa-Callejero L, Martinez A. Adrenomedullin and tumour microenvironment. J Transl Med. 2014;12:339.
4. Russell FA, King R, Smillie SJ, Kodji X, Brain SD. Calcitonin gene-related peptide: physiology and pathophysiology. Physiol Rev. 2014;94:1099–142.
5. Davis RB, Kechele DO, Blakeney ES, Pawlak JB, Caron KM. Lymphatic deletion of calcitonin receptor-like receptor exacerbates intestinal inflammation. JCI Insight. 2017;2:e92465.
6. Hershey AD. CGRP—the next frontier for migraine. N Engl J Med. 2017;377:2190–1.
7. Dodick DW Migraine. *Lancet* 2018;391:1315–30.
8. Berenguer-Daize C, Boudouresque F, Bastide C, Tounsi A, Benyahia Z, Acunzo J, et al. Adrenomedullin blockade suppresses growth of human hormone-independent prostate tumor xenograft in mice. Clin Cancer Res. 2013;19:6138–50.
9. Kaafarani I, Fernandez-Sauze S, Berenguer C, Chinot O, Delfino C, Dussert C, et al. Targeting adrenomedullin receptors with systemic delivery of neutralizing antibodies inhibits tumor angiogenesis and suppresses growth of human tumor xenografts in mice. FASEB J. 2009;23:3424–35.
10. Ouafik L, Sauze S, Boudouresque F, Chinot O, Delfino C, Fina F, et al. Neutralization of adrenomedullin inhibits the growth of human glioblastoma cell lines in vitro and suppresses tumor xenograft growth in vivo. Am J Pathol. 2002;160:1279–92.
11. Chen P, Huang Y, Bong R, Ding Y, Song N, Wang X, et al. Tumor-associated macrophages promote angiogenesis and melanoma growth via adrenomedullin in a paracrine and autocrine manner. Clin Cancer Res. 2011;17:7230–9.
12. Toda M, Suzuki T, Hosono K, Hayashi I, Hashiba S, Onuma Y, et al. Neuronal system-dependent facilitation of tumor angiogenesis and tumor growth by calcitonin gene-related peptide. Proc Natl Acad Sci USA. 2008;105:13550–5.
13. Harzenetter MD, Keller U, Beer S, Riedl C, Peschel C, Holzmann B. Regulation and function of the CGRP receptor complex in human granulopoiesis. Exp Hematol. 2002;30:306–12.
14. Chute JP, Muramoto GG, Dressman HK, Wolfe G, Chao NJ, Lin S. Molecular profile and partial functional analysis of novel endothelial cell-derived growth factors that regulate hematopoiesis. Stem Cells. 2006;24:1315–27.
15. Broome CS, Whetton AD, Miyan JA. Neuropeptide control of bone marrow neutrophil production is mediated by both direct and indirect effects on CFU-GM. Br J Haematol. 2000;108:140–50.
16. De Angeli S, Di Liddo R, Buoro S, Toniolo L, Conconi MT, Belloni AS, et al. New immortalized human stromal cell lines enhancing in vitro expansion of cord blood hematopoietic stem cells. Int J Mol Med. 2004;13:363–71.
17. Krug U, Berdel WE, Gale RP, Haferlach C, Schnittger S, Muller-Tidow C, et al. Increasing intensity of therapies assigned at diagnosis does not improve survival of adults with acute myeloid leukemia. Leukemia. 2016;30:1230–6.
18. Verhaak RG, Wouters BJ, Erpelinck CA, Abbas S, Beverloo HB, Lugthart S, et al. Prediction of molecular subtypes in acute

myeloid leukemia based on gene expression profiling. Haematologica. 2009;94:131–4.
19. Valk PJ, Verhaak RG, Beijen MA, Erpelinck CA, Barjesteh van Waalwijk van Doorn-Khosrovani S, Boer JM, et al. Prognostically useful gene-expression profiles in acute myeloid leukemia. N Engl J Med. 2004;350:1617–28.
20. The Cancer Genome Atlas Research Network. Genomic and epigenomic landscapes of adult de novo acute myeloid leukemia. N Engl J Med. 2013;368:2059–74.
21. Lavallee VP, Baccelli I, Krosl J, Wilhelm B, Barabe F, Gendron P, et al. The transcriptomic landscape and directed chemical interrogation of MLL-rearranged acute myeloid leukemias. Nat Genet. 2015;47:1030–7.
22. Herold T, Metzeler KH, Vosberg S, Hartmann L, Rollig C, Stolzel F, et al. Isolated trisomy 13 defines a homogeneous AML subgroup with high frequency of mutations in spliceosome genes and poor prognosis. Blood. 2014;124:1304–11.
23. Schuffler PJ, Fuchs TJ, Ong CS, Wild PJ, Rupp NJ, Buhmann JM. TMARKER: a free software toolkit for histopathological cell counting and staining estimation. J Pathol Inf. 2013;4(Suppl):S2.
24. Pabst C, Bergeron A, Lavallee VP, Yeh J, Gendron P, Norddahl GL, et al. GPR56 identifies primary human acute myeloid leukemia cells with high repopulating potential in vivo. Blood. 2016;127:2018–27.
25. Dohner H, Estey E, Grimwade D, Amadori S, Appelbaum FR, Buchner T, et al. Diagnosis and management of AML in adults: 2017 ELN recommendations from an international expert panel. Blood. 2017;129:424–47.
26. Zou H, Hastie T. Regularization and variable selection via the elastic net. J R Stat SocSer B (Stat Methodol). 2005;67:301–20.
27. Langer C, Marcucci G, Holland KB, Radmacher MD, Maharry K, Paschka P, et al. Prognostic importance of MN1 transcript levels, and biologic insights from MN1-associated gene and microRNA expression signatures in cytogenetically normal acute myeloid leukemia: a cancer and leukemia group B study. J Clin Oncol. 2009;27:3198–204.
28. Langer C, Radmacher MD, Ruppert AS, Whitman SP, Paschka P, Mrozek K, et al. High BAALC expression associates with other molecular prognostic markers, poor outcome, and a distinct gene-expression signature in cytogenetically normal patients younger than 60 years with acute myeloid leukemia: a Cancer and Leukemia Group B (CALGB) study. Blood. 2008;111:5371–9.
29. Schwind S, Marcucci G, Kohlschmidt J, Radmacher MD, Mrozek K, Maharry K, et al. Low expression of MN1 associates with better treatment response in older patients with de novo cytogenetically normal acute myeloid leukemia. Blood. 2011;118:4188–98.
30. Tanner SM, Austin JL, Leone G, Rush LJ, Plass C, Heinonen K, et al. BAALC, the human member of a novel mammalian neuroectoderm gene lineage, is implicated in hematopoiesis and acute leukemia. Proc Natl Acad Sci USA. 2001;98:13901–6.
31. Baldus CD, Thiede C, Soucek S, Bloomfield CD, Thiel E, Ehninger G. BAALC expression and FLT3 internal tandem duplication mutations in acute myeloid leukemia patients with normal cytogenetics: prognostic implications. J Clin Oncol. 2006;24:790–7.
32. Heuser M, Beutel G, Krauter J, Dohner K, von Neuhoff N, Schlegelberger B, et al. High meningioma 1 (MN1) expression as a predictor for poor outcome in acute myeloid leukemia with normal cytogenetics. Blood. 2006;108:3898–905.
33. Hattori A, Tsunoda M, Konuma T, Kobayashi M, Nagy T, Glushka J, et al. Cancer progression by reprogrammed BCAA metabolism in myeloid leukaemia. Nature. 2017;545:500–4.
34. Garrison BS, Rybak AP, Beerman I, Heesters B, Mercier FE, Scadden DT, et al. ZFP521 regulates murine hematopoietic stem cell function and facilitates MLL-AF9 leukemogenesis in mouse and human cells. Blood. 2017;130:619–24.
35. Ng SW, Mitchell A, Kennedy JA, Chen WC, McLeod J, Ibrahimova N, et al. A 17-gene stemness score for rapid determination of risk in acute leukaemia. Nature. 2016;540:433–7.
36. Stelljes M, Krug U, Beelen DW, Braess J, Sauerland MC, Heinecke A, et al. Allogeneic transplantation versus chemotherapy as postremission therapy for acute myeloid leukemia: a prospective matched pairs analysis. J Clin Oncol. 2014;32:288–96.
37. Marino R, Struck J, Maisel AS, Magrini L, Bergmann A, Di Somma S. Plasma adrenomedullin is associated with short-term mortality and vasopressor requirement in patients admitted with sepsis. Crit Care. 2014;18:R34.
38. Koyama T, Ochoa-Callejero L, Sakurai T, Kamiyoshi A, Ichikawa-Shindo Y, Iinuma N, et al. Vascular endothelial adrenomedullin-RAMP2 system is essential for vascular integrity and organ homeostasis. Circulation. 2013;127:842–53.
39. Nikitenko LL, Leek R, Henderson S, Pillay N, Turley H, Generali D, et al. The G-protein-coupled receptor CLR is upregulated in an autocrine loop with adrenomedullin in clear cell renal cell carcinoma and associated with poor prognosis. Clin Cancer Res. 2013;19:5740–8.
40. Martinez A, Vos M, Guedez L, Kaur G, Chen Z, Garayoa M, et al. The effects of adrenomedullin overexpression in breast tumor cells. J Natl Cancer Inst. 2002;94:1226–37.
41. Oehler MK, Hague S, Rees MC, Bicknell R. Adrenomedullin promotes formation of xenografted endometrial tumors by stimulation of autocrine growth and angiogenesis. Oncogene. 2002;21:2815–21.
42. Dong J, He Y, Zhang X, Wang L, Sun T, Zhang M, et al. Calcitonin gene-related peptide regulates the growth of epidermal stem cells in vitro. Peptides. 2010;31:1860–5.
43. Martinez-Herrero S, Larrayoz IM, Ochoa-Callejero L, Garcia-Sanmartin J, Martinez A. Adrenomedullin as a growth and cell fate regulatory factor for adult neural stem cells. Stem Cells Int. 2012;2012:804717.
44. Padro T, Ruiz S, Bieker R, Burger H, Steins M, Kienast J, et al. Increased angiogenesis in the bone marrow of patients with acute myeloid leukemia. Blood. 2000;95:2637–44.
45. Passaro D, Di Tullio A, Abarrategi A, Rouault-Pierre K, Foster K, Ariza-McNaughton L, et al. Increased vascular permeability in the bone marrow microenvironment contributes to disease progression and drug response in acute myeloid leukemia. Cancer Cell. 2017;32:324–41. e326.
46. Schepers K, Campbell TB, Passegue E. Normal and leukemic stem cell niches: insights and therapeutic opportunities. Cell Stem Cell. 2015;16:254–67.
47. Schliemann C, Bieker R, Padro T, Kessler T, Hintelmann H, Buchner T, et al. Expression of angiopoietins and their receptor Tie2 in the bone marrow of patients with acute myeloid leukemia. Haematologica. 2006;91:1203–11.
48. Dias S, Hattori K, Zhu Z, Heissig B, Choy M, Lane W, et al. Autocrine stimulation of VEGFR-2 activates human leukemic cell growth and migration. J Clin Invest. 2000;106:511–21.
49. Papaioannou D, Shen C, Nicolet D, McNeil B, Bill M, Karunasiri M, et al. Prognostic and biological significance of the proangiogenic factor EGFL7 in acute myeloid leukemia. Proc Natl Acad Sci USA. 2017;114:e4641–7.
50. Di Liddo R, Bridi D, Gottardi M, De Angeli S, Grandi C, Tasso A, et al. Adrenomedullin in the growth modulation and differentiation of acute myeloid leukemia cells. Int J Oncol. 2016;48:1659–69.
51. Kocemba KA, van Andel H, de Haan-Kramer A, Mahtouk K, Versteeg R, Kersten MJ, et al. The hypoxia target adrenomedullin is aberrantly expressed in multiple myeloma and promotes angiogenesis. Leukemia. 2013;27:1729–37.

52. Reuter U, Goadsby PJ, Lanteri-Minet M, Wen SH, Hours-Zesiger P, Ferrari MD, et al. Efficacy and tolerability of erenumab in patients with episodic migraine in whom two-to-four previous preventive treatments were unsuccessful: a randomised, double-blind, placebo-controlled, phase 3b study. Lancet. 2018;392: 2280–7.

Affiliations

Linus Angenendt[1] · Eike Bormann[2] · Caroline Pabst[3] · Vijay Alla[1] · Dennis Görlich[2] · Leonie Braun[1] · Kim Dohlich[1] · Christian Schwöppe[1] · Stefan K. Bohlander[4] · Maria Francisca Arteaga[1] · Klaus Wethmar[1] · Wolfgang Hartmann[5] · Adrian Angenendt[6] · Torsten Kessler[1] · Rolf M. Mesters[1] · Matthias Stelljes[1] · Maja Rothenberg-Thurley[7] · Karsten Spiekermann[7] · Josée Hébert[8,9,10,11] · Guy Sauvageau[8,9,10,11] · Peter J. M. Valk[12] · Bob Löwenberg[12] · Hubert Serve[13] · Carsten Müller-Tidow[3] · Georg Lenz[1] · Bernhard J. Wörmann[14] · M. Christina Sauerland[2] · Wolfgang Hiddemann[7] · Wolfgang E. Berdel[1] · Utz Krug[15] · Klaus H. Metzeler[7] · Jan-Henrik Mikesch[1] · Tobias Herold[7,16] · Christoph Schliemann[1]

[1] Department of Medicine A, University Hospital Münster, Münster, Germany

[2] Institute of Biostatistics and Clinical Research, University of Münster, Münster, Germany

[3] Department of Medicine V, University Hospital Heidelberg, Heidelberg, Germany

[4] Leukaemia & Blood Cancer Research Unit, Department of Molecular Medicine and Pathology, University of Auckland, Auckland, New Zealand

[5] Gerhard-Domagk-Institute of Pathology, University Hospital Münster, Münster, Germany

[6] Department of Biophysics, Faculty of Medicine, Centre for Integrative Physiology and Molecular Medicine (CIPMM), Saarland University, Homburg, Germany

[7] Department of Medicine III, University Hospital Grosshadern, LMU Munich, Munich, Germany

[8] The Leucegene Project at Institute for Research in Immunology and Cancer, University of Montreal, Montreal, QC, Canada

[9] Division of Hematology-Oncology, Maisonneuve-Rosemont Hospital, Montreal, QC, Canada

[10] Quebec Leukemia Cell Bank, Maisonneuve-Rosemont Hospital, Montreal, QC, Canada

[11] Department of Medicine, University of Montreal, Montreal, QC, Canada

[12] Department of Hematology, Erasmus University Medical Centre, Rotterdam, The Netherlands

[13] Department of Hematology and Oncology, University Hospital Frankfurt, Frankfurt, Germany

[14] Department of Hematology, Oncology and Tumor Immunology, Charité University Medicine, Campus Virchow, Berlin, Germany

[15] Department of Medicine 3, Klinikum Leverkusen, Leverkusen, Germany

[16] Research Unit Apoptosis in Hematopoietic Stem Cells, Helmholtz Zentrum München, German Center for Environmental Health (HMGU), Munich, Germany